Cavity opening by a giant planet in a protoplanetary disc and effects on planetary migration

A. Crida, A. Morbidelli

Mon. Not. R. Astron. Soc. **377,** 1324–1336 (2007) doi:10.1111/j.1365-2966.2007.11704.x

Cavity opening by a giant planet in a protoplanetary disc and effects on planetary migration

A. Crida⋆ and A. Morbidelli
O.C.A., B.P. 4229, 06304 Nice Cedex 4, France

Accepted 2007 March 6. Received 2007 March 2; in original form 2007 January 24

ABSTRACT

We study the effect of a Jovian planet on the gas distribution of a protoplanetary disc, using a new numerical scheme that allows us to take into consideration the global evolution of the disc, down to an arbitrarily small inner physical radius. We find that Jovian planets do not open cavities in the inner part of the disc (i.e. interior to their orbits) unless (a) the inner physical edge of the disc is close to the planet's location or (b) the planet is much more massive than the disc. In all other cases the planet simply opens a gap in the gas density distribution, whose global profile is essentially unchanged relative to the one that it would have if the planet were absent. We recognize, though, that the dust distribution can be significantly different from the gas distribution and that dust cavities might be opened in some situations, even if the gas is still present in the inner part of the disc.

Concerning the migration of the planet, we find that classical type II migration (with speed proportional to the viscosity of the disc) occurs only if the gap opened by the planet is deep and clean. If there is still a significant amount of gas in the gap, the migration of the planet is generally slower than the theoretical type II migration rate. In some situations, migration can be stopped or even reversed. We develop a simple model that reproduces satisfactorily the migration rate observed in the simulations, for a wide range of disc viscosities and planet masses and locations relative to the inner disc edge. Our results are relevant for extrasolar planetary systems, as they explain (a) why some hot Jupiters did not migrate all the way down to their parent stars and (b) why the outermost of a pair of resonant planets is typically the most massive one.

Key words: accretion, accretion discs – Solar system: formation – planetary systems: formation – planetary systems: protoplanetary discs.

1 INTRODUCTION

The planet–disc interactions have been subject of an increased interest since the discovery of the first exoplanet (Mayor & Queloz 1995). Indeed, the first extrasolar planets discovered were giant gaseous planets orbiting surprisingly close to their parent star, so that they are called *hot Jupiters*. According to classical planetary formation models in protoplanetary discs (Pollack et al. 1996), hot Jupiters could not form where they currently orbit, because there was not enough solids to build a massive core that would accrete a gaseous atmosphere (there is much more solid material beyond the so-called 'snow line' where water condensates into ice). In addition, gas heated by the star is more difficult to capture for the solid core than cold gas. It has been shown by Bodenheimer, Hubickyj & Lissauer (2000) that *in situ* formation of hot Jupiter is not impossible, but it is not the most likely scenario. This suggests that the planets migrate in the disc via angular momentum exchanges with the gas.

In fact, the planet always exerts a positive torque on the part of the disc outside its orbit, and a negative one on the part of the disc inside its orbit (Goldreich & Tremaine 1979; Lin & Papaloizou 1979; Ward 1997). Reciprocally the disc exerts the opposite torques on the planet; if the disc density profile is not perturbed by the planet, the sum of the torques is not zero but results in the so-called *differential Lindblad torque*, which is negative and responsible for the inward *type I migration* (Ward 1997). However, the torques exerted by the planet on the disc tend to repel the gas away from the planetary orbit; whether the internal stress in the disc is strong enough to counterbalance this planetary torque and spread the gas into the void regions determines whether the corotation region of the planet is depleted or not, leading to the opening of a more or less clean *gap*. For more detail on the gap opening process, we refer to Crida et al. (2006) and references therein; the basic idea is that the

⋆E-mail: crida@oca.eu

density profile evolves in response to the presence of the planet, in order to achieve an equilibrium among three torques exerted on a fluid element. These torques are due to the gravity of the planet and to the viscosity and the pressure in the gas; the two latter ones depend strongly on the gas density profile. The stronger is the planetary torque (it is proportional to the planet mass) the steeper has to be the density profile, and thus the deeper is the gap.

If a clean gap is opened, the planet is locked into it because the outer and the inner disc are repellent for the planet. Thus, the planet is supposed to follow the viscous evolution of the disc (accretion on to the central star and viscous spreading, see Lynden-Bell & Pringle 1974, hereafter LP74); this is the definition of *type II migration*. However, Quillen et al. (2004) noticed that if the planet is more massive than the inner disc, the outer disc is not able to push the planet inward at the speed of the natural gaseous accretion on to the star. Indeed, in that case the planet has more angular momentum to lose than the unperturbed disc would have, so that it migrates more slowly. Meanwhile, nothing prevents the inner disc from accreting on to the star. Even more, Varnière et al. (2006) suggested that, as the planet exerts a negative torque on the inner disc, it accelerates the accretion of the latter on to the primary. Consequently, the inner disc accretes on to the central star faster than it would naturally. This makes the inner disc disappear before the planet migrates inward. The result is the opening of a *cavity*: a great depletion of the disc from the star to the planet's orbit.

Once a cavity is opened, the outer disc still tends to accrete on to the central star and to push the planet inward, while the planet cannot take angular momentum from the inner disc anymore. A big mass of the planet with respect to the disc may slow down this process, but the final result should ineluctably be the inward type II migration of the planet toward the star. Reality, however, is not so simple. In fact, in this work we will show that, under some conditions on the gas disc viscosity, the orbit of the planet is not 'gasproof' and viscous accretion can happen without forcing the migration of the planet.

The cavity opening process and its feedback on planet migration are not easy to study and quantify with the help of numerical simulations. Indeed, the computation of the inner disc evolution is prohibitive with classical hydrocodes. Thus, Quillen et al. (2004) only made the simulation of a planet orbiting inside a pre-existing cavity – showing that it did not migrate inward very fast – and Varnière et al. (2006) performed only a few simulations showing the opening of a cavity by a Jupiter mass planet in a low-density disc. The cavity opening appeared to be more rapid than the viscous time-scale, confirming the idea that the planet 'helps' the accretion of the inner disc on to the star. However, Varnière et al. (2006) did not provide an exploration of the parameter space, and could not study the planetary migration because the planet was about 100 times more massive than the disc. With the help of a new numerical scheme that simulates efficiently and realistically the inner disc evolution (Crida, Morbidelli & Masset 2007), we can perform such a study for the first time. This is the main scope of this paper. This analysis is particularly interesting because observations suggest that some protoplanetary discs most likely host cavities. Understanding what kind of cavity a planet can open in terms of size, shape and depth, in which conditions and with which lifetime, may provide some keys to interpret these observations. We also stress that the ALMA interferometer will enable us to make precise images of the inner part of protoplanetary discs. In this frame, it is relevant to study the features resulting from planet–disc interactions that might be observed.

In Section 2, we will shortly review the observations of protoplanetary discs that seem to host cavities. After a brief description of the algorithm used for our numerical simulations (Section 3), we present the results in Section 4 in terms of cavity opening and migration. These numerical experiments are interpreted in Sections 5 and 6 with a semi-analytical model. We discuss in particular the survivability of a cavity opened by a planet with regard to type II migration, and we find that the corotation torque can prevent this inward migration. In Section 8 we discuss the difference between gas cavities and dust cavities. Finally, we conclude and discuss the implications of this work in Section 9.

2 EVIDENCES FOR CAVITIES IN PROTOPLANETARY DISCS

Discs of gas and dust around young stars are heated by the star and by internal viscous dissipation. Consequently, the dust becomes an infrared (IR) source. In the spectral energy distribution (SED) of the star, an IR excess reveals the presence of such a disc. The near-IR (NIR) emission corresponds to the hottest part of the disc, which is the closest to the central star, while the mid-IR emission is due to colder dust, corresponding to the outer part of the disc. Consequently, a lack of IR excess in the NIR part of the spectrum can be interpreted as the presence of an inner cavity in the disc (Beckwith 1999). Such a cavity discovered by SED analysis is sometimes called a *spectral hole*.

One of the most clear examples of spectral hole is given in fig. 2 of Forrest et al. (2004) for the T-Tauri star CoKu Tau/4 observed with the *Spitzer* telescope. The size of the spectral hole is such that there seems to be no dust at temperature larger than 123 K. The authors convincingly deduce from this SED that dust grains in the disc of CoKu Tau/4 are excluded from the innermost 10 au; this makes a remarkable dust cavity. The question whether this cavity could be opened and maintained by a planet has been addressed in Quillen et al. (2004). They suppose that a planet opened a gap in the disc at 10 au, and that the inner disc subsequently accreted on to the star. Then the age of the system has to be bigger than the viscous time-scale of accretion on to the star of the inner disc. This gives a lower limit for the viscosity. Given the viscosity, a minimum planet mass is required to open a gap. For the planet not to migrate immediately after the depletion of the inner disc, the planet has to be more massive than the outer disc, so that the angular momentum taken by the latter from the planet is a negligible fraction of the angular momentum of the planet. From these considerations, Quillen et al. performed a simulation with a planet of mass $3 \times 10^{-4} M_*$ on a circular orbit at 10 au in a disc with Reynolds number 10^5 and density $\Sigma(r) = 10^{-6}$ $(1.1 r_\mathrm{p}/r) M_*\,\mathrm{au}^{-2}$ for $r > 1.1 r_\mathrm{p}$ and 100 times smaller for smaller radii. The planet efficiently maintained the cavity for the duration of the simulation (100 orbits). However, they did not make a simulation of the process of cavity opening.

The T-Tauri stars TW Hya, DM Tau and GM Aur also present a spectral hole. To interpret their SEDs, Calvet et al. (2002, 2005) used the following model. They divided the disc into three components: an optically thick outer disc, its inner edge (represented as a wall directly exposed to stellar radiations) and an optically thin inner region. Adjusting the free parameters (the wall radius and height, the outer disc scaleheight, its mass and viscosity) they obtained a satisfactory fit of the SED of these three objects. They concluded that TW Hya and DM Tau present a 3–4 au wide cavity, while GM Aur should have the truncation radius of the outer disc located at 24 au from the star. Previous work on GM Aur (Bergin et al. 2004) based on different data, concluded that the cavity is 6-au wide. Such a cavity could be maintained by a 1.7 Jupiter mass planet on a fixed circular orbit at 2.5 au (Rice et al. 2003).

Dullemond, Dominik & Natta (2001) proposed a different model for the SED of Herbig Ae stars that does not involve the presence of a planet. In their model, the inner part of the disc is removed, so that the inner rim is directly exposed to stellar radiations. It is thus heated a lot, and gets puffed up. This has two consequences: first, this rim is a strong IR source, leading to a peak at 2–3 μm in the SED; second, the disc behind the puffed up inner rim is in the shadow. Thus, this region remains cold and does nearly not radiate in IR. If the disc is flared, however, the outermost part of the disc can be lightened by the star, and then becomes an IR source. In that case, the SED presents a gap between the peak at 2–3 μm due to the hot rim and the emission of the outer disc at larger wavelength, because it is colder. This is in good agreement with the SED of the Herbig Ae star AB Aur, with a rim of height 0.1 at 0.52 au (which corresponds to the dust sublimation radius).

More recently, interferometric observations at Plateau de Bure Interferometer clearly showed a remarkable dust depletion in the inner 50 au of the disc of LkCa15 (Piétu et al. 2006). The possibility that a massive planet or a brown dwarf is responsible for this is work in progress and will be addressed in a forthcoming paper.

Thus, cavities are relatively common features in protoplanetary discs. It is not easy to constrain their characteristics, as sometimes different dust distributions can give indiscernible SEDs, but the evidence for cavities in protoplanetary discs is quite strong.

3 NUMERICAL SIMULATIONS SET-UP

Classical hydrocodes for the simulation of planet–disc interactions represent the disc with a two-dimensional (2D) polar grid extending between an inner and an outer radius ($R_{\rm in}^{\rm 2D}$ and $R_{\rm out}^{\rm 2D}$). The grid covers the planetary region and, provided that the resolution is good enough, satisfactorily describes the local planet–disc interactions. The grid cannot reasonably cover the full disc, for the following reasons. First, a prohibitive number of cells would be required to extend the grid from the planet region (a few astronomical units from the star) to the physical outer edge of the disc (often located at several hundreds of astronomical units from the star). Second, and more important, the simulation of the inner part of the disc requires a shortage of the time-step and an increase of CPU time roughly proportional to $\Omega_{\rm max}^{-1} \propto (R_{\rm in}^{\rm 2D})^{-3/2}$ in most codes, where Ω is the angular velocity. Because the grid covers only a portion of the disc, the global evolution of the disc cannot be realistically described. Yet, it is the global evolution of the disc that governs type II migration. Thus, the accuracy of the type II migration observed in simulations can be questioned. Another point related to the global evolution of the disc is the evolution of its innermost part and its accretion on to the star, that is the opening of a cavity. Consequently, it seems that classical hydrocodes are not adapted for the study of these two problems on which we wish to focus. We developed an improvement to the classical algorithm that we briefly present below.

3.1 Code description

The code used for this work is based on the hydrocode FARGO (Masset 2000a,b). To describe correctly the evolution of the disc outside the 2D grid, we add a one-dimensional (1D) grid extended all over the physical disc, from its inner edge (the radius of the central star or the X-wind truncation radius) to its outer edge. This non-azimuthally resolved grid is coupled to the 2D grid at the boundaries of the latter in a conservative way. Thanks to this coupling, the disc perturbations due to the planet – computed locally in the 2D grid in FARGO – influence the global evolution described in the 1D grid; this evolution in turn affects the computation in the 2D grid as it provides realistic, time-evolving boundary conditions for the latter. This numerical scheme, described in Crida et al. (2007), enables us to simulate the type II migration with an excellent reliability as well as the accretion of the inner disc on to the star, for a negligible additional computing cost with respect to a classical 2D hydrocode.

3.2 Units and parameters

The central star mass is set equal to $\rm M_\odot$, which is our mass unit. As length unit, we adopt the astronomical unit (au), and we set for simplicity the gravitational constant $G = 1$ (so that 1 yr lasts 2π time units).

The initial density profile corresponds to a disc that evolved for some time under the effect of its own viscosity and was provided by Guillot & Hueso (2006). It can be approximated by

$$\Sigma(r) \approx 10^{-5}\ \exp(-r^2/1320). \quad (1)$$

This initial density corresponds to the minimal-mass solar nebula (Hayashi 1981) at the location of Jupiter (5.2 au). The aspect ratio H/r is constant in space and time; its default value is 0.05. These parameters (density and aspect ratio) will be changed in some test runs to study their influence on the results. The sound speed is $c_{\rm s} = H\Omega$, where H is the height of the disc. The equation of state is isothermal (the pressure is $P = \rho c_{\rm s}^2$, where ρ is the volume density, so that it becomes $P = \Sigma c_{\rm s}^2$ in our 2D formalism, after integration on the disc's scaleheight).

If not specified otherwise, in most of the runs the 2D grid extends radially from $R_{\rm in}^{\rm 2D} = 1.75$ to $R_{\rm out}^{\rm 2D} = 15$ au and is divided in $N_{\rm r} = 165$ elementary rings, themselves divided into $N_{\rm s} = 320$ sectors. The 1D grid extends radially from 0.58333 to 100 au, over $N_{\rm r}^{\rm 1D} = 1193$ elementary rings.

4 RESULTS

We computed a few simulations with a Jupiter mass planet ($q = M_{\rm p}/M_* = 10^{-3}$) initially placed on a circular orbit at $r_{\rm p} = 5$ au in a disc with different viscosities. The kinematic viscosity of the gas, ν, is constant in space and time. Its values in the simulations are such that the Reynolds number at the initial location of the planet ($\mathcal{R} = {r_{\rm p}}^2\Omega_{\rm p}/\nu$) goes from $10^{3.8}$ to 10^6.

4.1 Density profile and cavity opening

Fig. 1 shows with bold lines the density profiles for four simulations after half a viscous time ($t_\nu = r_{\rm p}^2\nu^{-1}$), or only a quarter of viscous time in the least viscous case. The depth of the gap opened by the planet strongly depends on the Reynolds number. This is not surprising, as it is well known that viscosity plays against gap opening (see for instance Crida et al. 2006, and references therein). The gap is centred on the planetary orbit, which is not any more at 5 au because the planet has migrated.

Concerning the opening of a cavity, we see that the density in the inner disc is significantly smaller than in the outer disc. In particular, the least viscous cases show an inner disc with very low density, so that a sort of cavity is formed: in fact, the density is about five times smaller for $r < 2.5$ than for $r > 3$. The profile clearly shows a wall at $r \approx 2.5$, beyond which the disc profile is about flat while the density is negligible at the base of the wall.

The thin dotted lines show the density profile obtained in similar simulations, at the same time, in the same conditions, but without the planet. The density also decreases in the innermost region of the

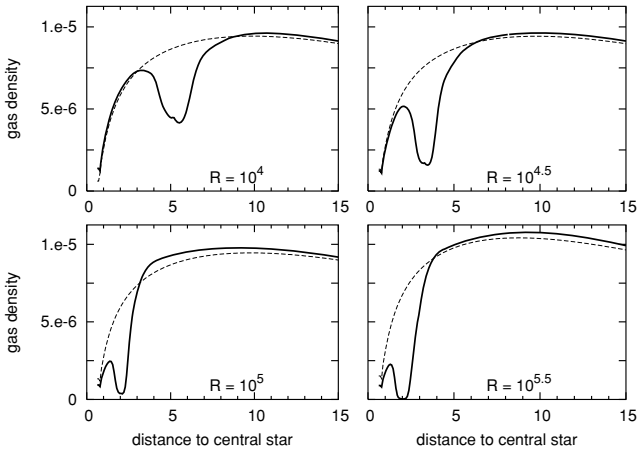

Figure 1. Bold lines: surface density profile at $t_\nu/2$, for different Reynolds number, labelled on the corresponding panel. For $\mathcal{R} = 10^{5.5}$, the time is $t_\nu/4$. Thin dashed lines: surface density profile at the same times for a similar disc with no planet. The units of mass and length are those specified in Section 3.2: solar mass and astronomical unit.

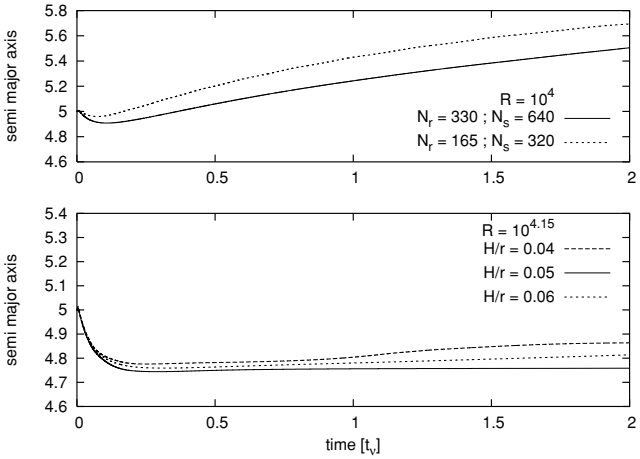

Figure 3. Top panel: outward migration of a Jupiter mass planet for $\mathcal{R} = 10^4$ and two different resolutions. Bottom panel: quasi-stationary evolution of a Jupiter mass planet for $\mathcal{R} = 10^{4.15}$ and three different aspect ratios.

disc. So, it seems that the observed depletion of the inner disc is not fully caused by the planet, as will be discussed in Section 5.

4.2 Migration rate

Fig. 2 shows the evolution of the semimajor axis of the planet with time, in units of the viscous time t_ν. In proper type II migration, the migration rate is proportional to the viscosity and thus, in this time unit, it should be independent of $\mathcal{R}$. This is indeed the case for $\mathcal{R} \geqslant 10^5$: the three curves are almost linear and overlap, at least in the first part of the evolution. However, for higher viscosities, a very different behaviour is observed. When $\mathcal{R}$ decreases below 10^5, the migration rate becomes slower than expected. As viscosity increases, the planets migrates inward more and more slowly with respect to the viscous time, and the migration is even stopped for $\mathcal{R} = 10^{4.15}$. We will refer to this case hereafter as the *stationary case*. For larger viscosities, the migration is reversed and the planet moves outward.

This result is particularly surprising and new. This outward migration is not an effect of the resolution of the grid; we have recomputed the simulation with $\mathcal{R} = 10^4$, using $N_\mathrm{r} = 330$, $N_\mathrm{s} = 640$: the planet also migrates outward, at about the same speed (see top panel in Fig. 3). With this high resolution, the size of a cell around the planet is about a tenth of the Hill radius in radius and a seventh of the Hill radius in azimuth, so that the Hill sphere of the planet is covered by about 220 cells. This is largely sufficient; in particular the corotation zone of the planet, which plays a crucial role as will be shown further, is correctly simulated. We also investigated the effect of the aspect ratio on the migration rate, from the stationary case. It appears that this parameter only plays a marginal role (see bottom panel in Fig. 3).

One may wonder if the stationary case observed for $\mathcal{R} = 10^{4.15}$ for a Jupiter mass planet is a feature valid for any planet mass. Fig. 4 shows that it is not the case. The more massive is the planet the faster it migrates inward, approaching the classical type II regime. For planets lighter than Jupiter, the migration is directed outward. However, there is a stationary orbit further from the star to which these low-mass planets tend, asymptotically; this will be shown in Fig. 6.

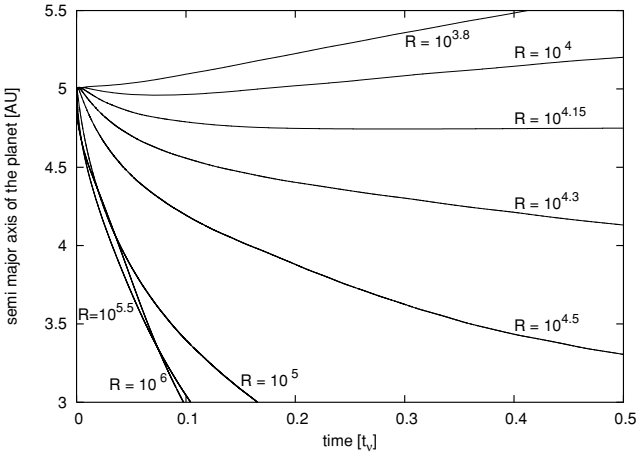

Figure 2. Migration of a Jupiter mass planet for different Reynolds numbers of the disc.

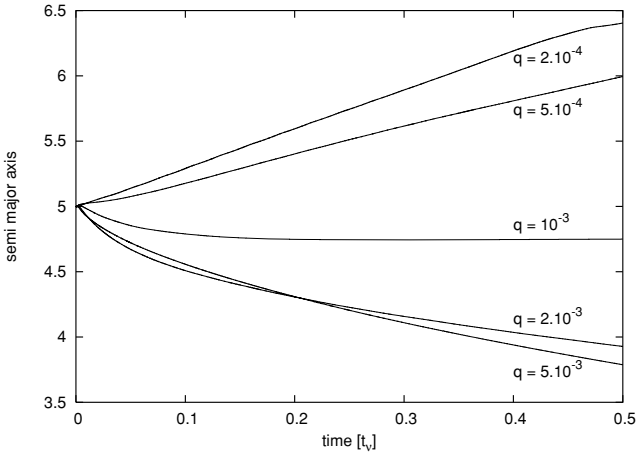

Figure 4. Migration of giant planets of different masses in a disc with $\mathcal{R} = 10^{4.15}$ and $H/r = 0.05$.

5 MODELLING THE DENSITY PROFILE

In this section we build a model to understand the shaping of the disc density profiles observed in Fig. 1. Our approach is done in three steps. First, we review the global viscous evolution of a disc that is not perturbed by any planet; then, we discuss how a gap is opened by a massive planet and finally we analyse in which situations the resulting density profile may show a significant depletion (a 'cavity') in the full inner part of the disc, up to the planetary orbit.

5.1 Global disc's viscous evolution

The natural viscous evolution of a gaseous disc is described in LP74. Using their partial differential equation (14), one can compute, with a step-by-step integration, the evolution of any initial profile. If the initial profile has a Gaussian shape ($\Sigma(r) = \Sigma_0 \exp(-ar^2)$, where a is an arbitrary constant), there is an explicit solution, given by equations (18) and (18′) of LP74. The initial shape is conserved, the surface density being

$$\Sigma(r) = \Sigma_0 T^{-5/4} \exp\left(-\frac{ar^2}{T}\right),$$

where $T = 12a\nu t + 1$.

This solution is valid only for a disc extending between 0 and infinity in radius. However, the inner radius of the disc, $R_{\rm inf}$, is never 0; it is at least the radius of the central star, most likely the corotation radius at a few tenth of astronomical units where the lines of the magnetic field reconnect (the so-called X-point; Shu et al. 1997). It could even be bigger, in the case of jet-emitting disc (JED): indeed, at the base of the jet, which may be several astronomical units large (Bacciotti et al. 2003; Coffey et al. 2004), accretion is dominated by the torque exerted by the jet and is much larger than the standard accretion; so, the outer radius of the jet could be considered as the inner open boundary of the standard disc. The explicit solution of the LP74 equations with a finite inner edge of the disc comes from equation (25) of LP74. With our units ($G = M_* = 1$), it gives

$$\Sigma_{\rm LP74}(r,t) = \Sigma_0 T^{-5/4} \left(\frac{\sqrt{r} - \sqrt{R_{\rm inf}}}{\sqrt{r}}\right) \exp\left(-\frac{ar^2}{T}\right). \quad (2)$$

Thus the density starts from 0 at $r = R_{\rm inf}$ and grows with r until $r \gg R_{\rm inf}$, where a classical Gaussian shape is reached. This kind of profile is illustrated by the thin dashed lines in Fig. 1. Fig. 5 shows the agreement between the disc profiles obtained for various viscosities in numerical simulations and the theoretical profile given by equation (2) with $\Sigma_0 = 1.224 \times 10^{-5}$ and $a = 1/1320$ at $t_\nu/2$ (i.e. $T = 1.114$). All profiles overlap with each other. This shows that, once the time is renormalized relative to the viscous time, the evolution of the disc density distribution is independent of the Reynolds number. Furthermore, it shows the excellent agreement between equation (2) and the numerical solution achieved with our simulation scheme. The little discrepancy visible in Fig. 5 comes from the fact that the original profile in the simulations is not given by equation (2) at $T = 1$ but by equation (1).

5.2 Gap opening in an evolving disc

Equation (14) of Crida et al. (2006) provides a way of computing semi-analytically the density profile of a gap for any disc and planet parameters. This equation comes from the equilibrium between the torques due to the gravity of the planet, the viscosity and the pressure in the disc. It applies outside the corotation zone of the planet, which approximately extends on each side of the orbit over a width $x_{\rm s}^+ \approx x_{\rm s}^- \approx 2R_{\rm H}$, where $R_{\rm H}$ is the Hill radius of the planet. The equation reads

$$\frac{R_{\rm H}}{\Sigma}\frac{{\rm d}\Sigma}{{\rm d}r} = \frac{0.35q^2\mathcal{R}{r_{\rm p}}^3 r\Delta^{-4}{\rm sgn}(\Delta) - (3/4)(\Omega/\Omega_{\rm p})}{(H/r)^2(r/r_{\rm p})\mathcal{R}a'' + (3/2)(r/R_{\rm H})(\Omega/\Omega_{\rm p})}, \quad (3)$$

where $a'' = (1/8)|\Delta/R_{\rm H}|^{-1.2} + 200\,|\Delta/R_{\rm H}|^{-10}$ and $\Delta = r - r_{\rm p}$.

Notice that a boundary condition is needed to solve this differential equation with a step-by-step procedure. The solution of this equation corresponds to the gap profile $\Sigma(r)$ in an ideal disc in steady state, under the influence of a non-migrating planet. Without the presence of the planet, the unperturbed profile of such a disc would be proportional to $r^{-1/2}$ because ν is assumed to be constant over r. Thus, to compute the profile in the inner part of the disc, we start from $\Sigma = \Sigma_0/\sqrt{R_{\rm inf}}$ at $r = R_{\rm inf}$ and we compute the density step-by-step until $r^- = r_{\rm p} - x_{\rm s}^-$. For the outer disc, we start with $\Sigma = \Sigma_0/\sqrt{R_{\rm sup}}$ at $r = R_{\rm sup}$ and follow equation (3) down to $r^+ = r_{\rm p} + x_{\rm s}^+$. Unfortunately, $\Sigma(r^-)/\sqrt{r^-}$ is not necessarily equal to $\Sigma(r^+)/\sqrt{r^+}$. Thus, we choose the lowest of these two values, say the one at r^-, and adjust the outer edge of the gap at $r^+ + \delta$, with δ such that $\Sigma(r^+ + \delta)/\sqrt{r^+ + \delta} = \Sigma(r^-)/\sqrt{r^-}$. As shown in Crida et al. (2006), this procedure gives a satisfactory approximation of the gap depth.

The use of equation (3) as explained above provides the gap profile in a disc whose unperturbed profile is $\Sigma(r) = \Sigma_0 r^{-1/2}$. Thus, multiplying this gap profile by $\sqrt{r}/\Sigma_0$ gives the gap profile in terms of fraction of the unperturbed profile. Let us denote $\sigma(r)$ this *fractional profile*. We think that it is reasonable to assume that the fractional profile is independent of the unperturbed profile. This is supported by Fig. 1, which shows that the planet opens a gap in the natural profile of the disc, without essentially changing it. Consequently, as a simple model of the gap profile in an evolving disc, we suggest that the unperturbed profile given by equation (2) can be multiplied by the fractional profile, obtaining

$$\Sigma(r) = \sigma(r)\Sigma_{\rm LP74}(r,t). \quad (4)$$

Fig. 6 displays this model in the $\mathcal{R} = 10^{4.15}$ case. The secondary panel shows the fraction profile $\sigma(r)$. In the main plot, the dashed line shows the unperturbed profile $\Sigma_{\rm LP74}(r,t)$ at $t = t_\nu/2$. The gap profiles from the numerical simulation at the same time (thin line) and from equation (4) (bold line) are compared. The agreement is quite satisfactory, in particular if one keeps in mind that we only have

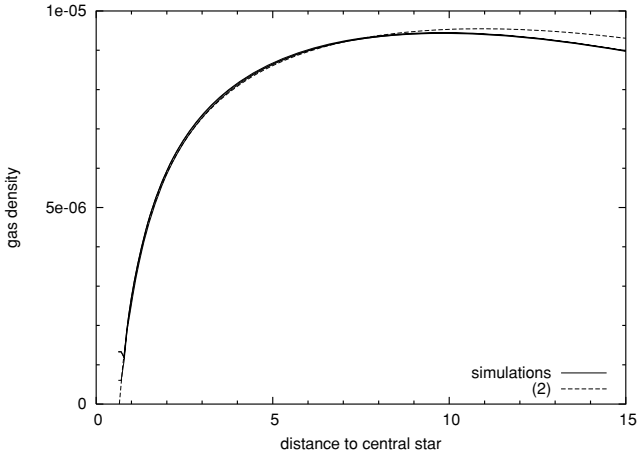

Figure 5. Surface density profile of an unperturbed disc at $t = t_\nu/2$. Plain lines: profiles from simulations with $\mathcal{R} = 10^4$, $10^{4.5}$ and 10^5. Dashed line: profile from equation (2).

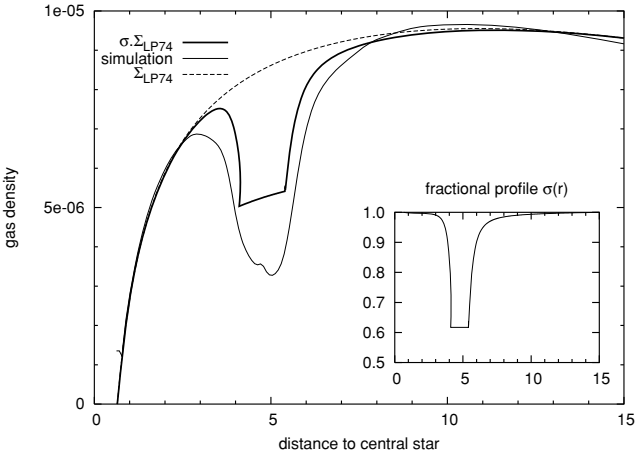

Figure 6. Gap profile in an evolving disc with $\mathcal{R} = 10^{4.15}$: the thin line results from numerical simulation while the bold line comes from our simple model. Dashed line: the unperturbed profile $\Sigma_{\rm LP74}(r,\, t_\nu/2)$ from equation (2). Secondary panel: 'fraction profile' $\sigma(r)$ of the gap deduced from equation (3).

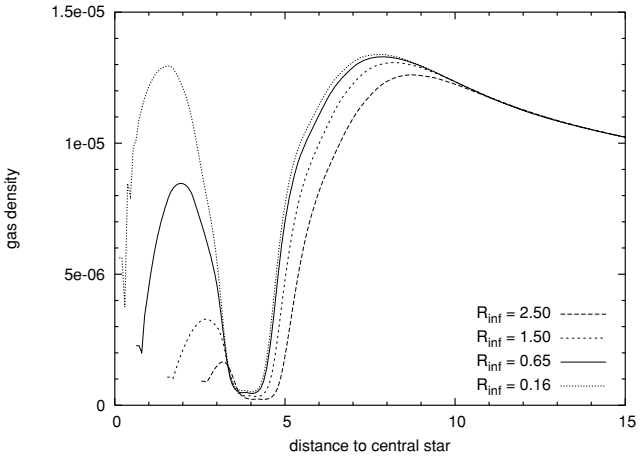

Figure 7. Density profiles obtained in numerical simulations at $t = t_\nu/10$ for discs with $\mathcal{R} = 10^5$ and different values of $R_{\rm inf}$.

a semi-analytic estimate of the gap profile. Indeed, as discussed in Crida et al. (2006), equation (3) provides gap profiles that are a bit too narrow and shallow for $\mathcal{R} \leqslant 10^5$ (while it provides slightly too wide and deep gaps for $\mathcal{R} > 10^{5.5}$). This is observed here as well. However, the gap edges in the model correspond quite well to the ones from the simulation in terms of position and slope. In addition, the profiles in the inner and outer disc nearly match those observed in the simulation.

We present here only this case, corresponding to a non-migrating planet. In the cases of a migrating planet, the situation is similar. This shows that this simple idea of multiplying the unperturbed profile by a schematic gap profile is valid in first approximation. As a matter of fact, a slight depletion of the inner disc with respect to the unperturbed profile is visible for cases with inward migrating planets. We will explain this in Section 7, after having developed a model that reproduces the migration rates.

5.3 Cavity opening

As we have seen above the disc density profile can be described effectively as the product of the fractional gap profile with the profile described by equation (2). This equation gives profiles which are proportional to $(1 - (r/R_{\rm inf})^{-1/2})\exp(-ar^2/T)$. The first term is about 1 for $r > 30\, R_{\rm inf}$, so that the profile at large radius is about Gaussian. However, for $r/R_{\rm inf} < 5$, the first term shapes the profile growing from 0 at $r = R_{\rm inf}$, with a slope proportional to $(r/R_{\rm inf})^{-3/2}$. Thus, it seems that $R_{\rm inf}$ is a key parameter for the profile of the innermost part of an evolving disc (see also Lubow & D'Angelo 2006).

Fig. 7 shows the density profiles at $t = t_\nu/10$ for discs with $\mathcal{R} = 10^5$ and four different values of $R_{\rm inf}$, as they result from numerical simulations. The plain line corresponds to $R_{\rm inf} = 0.65$ au as before (nominal case). The dotted line corresponds to a four times smaller value of $R_{\rm inf}$. All other parameters are the same in the two simulations. In both cases, the Jupiter mass planet has opened a gap in the disc and migrated down to $r_{\rm p} \approx 3.85$. The outer disc profiles almost overlap. The inner disc profiles, however, present a huge difference: the maximum density is nearly twice bigger in the small $R_{\rm inf}$ case than in the nominal $R_{\rm inf}$ case. In the nominal case, the inner disc is being depleted and a cavity is appearing. In the small $R_{\rm inf}$ case, there is only a gap. The tendency to the opening of deeper cavities with larger $R_{\rm inf}$ is confirmed in the last two simulations (short dashed and long dashed curves, respectively, in Fig. 7).

In conclusion, depending on the width and shape of the gap and on the position of the planet $r_{\rm p}$ with respect to the inner edge of the disc $R_{\rm inf}$, the density profile may show a cavity or not. Indeed, if the inner edge of the gap falls in the flat profile zone ($r \gtrsim 10\, R_{\rm inf}$), a classical gap is shaped (case $\mathcal{R} = 10^4$ in Fig. 1 and case $R_{\rm inf} = 0.16$ in Fig. 7). If it falls between 0 and $\sim 4\, R_{\rm inf}$, the density in the inner disc cannot grow enough before that the inner edge of the gap is reached and the planet seems to open a cavity (case $\mathcal{R} = 10^{5.5}$ in Fig. 1). Thus, the main parameter to determine whether a planet opens a cavity or not is the ratio between $r_{\rm p}$ and $R_{\rm inf}$. This should be taken into account in the interpretation of numerical simulations. To perform realistic simulations, it is necessary to have a realistic value of $R_{\rm inf}$. Thus, our code with coupled 2D and 1D grids (Crida et al. 2007) seems to be a tool of choice as it can handle arbitrarily small $R_{\rm inf}$.

Our result differs from the one by Varnière et al. (2006). They claimed that the depletion of the inner disc was faster than viscous because of the negative torque exerted by the planet. However, a planet in equilibrium in the middle of the gap simply transfers to the inner disc the torque that it feels from the outer disc; otherwise, the planet would move with respect to the gap. More precisely, in type II migration, the planet generally feels a total negative torque, and migrates inward, together with the disc and the gap; thus, the negative torque that the planet exerts on the inner disc is a bit *smaller* in magnitude than the one it feels from the outer disc. The difference corresponds to the loss of angular momentum of the planet. In the absence of the planet, there would be gas in the gap; this gas would also feel a negative torque from the outer disc, exert a smaller negative torque on the inner disc and migrate inward losing angular momentum. If the planet has the same mass as the gas that was initially in the gap, it has exactly the same effect on the disc. Consequently, we believe that the presence of the planet does not modify substantially the evolution of the inner disc – except maybe if the planet is much more massive than the disc, which was indeed the case in Varnière et al. (2006) analysis. This is confirmed in our simulations (see Section 7).

6 MODELLING THE MIGRATION RATE

It seems quite logical that, when the planet opens a clean gap, its migration follows a proper type II regime. With a Jupiter mass planet and a disc aspect ratio of 0.05, this happens for $\mathcal{R} > 10^5$ (see Figs 1 and 2).

However, for smaller Reynolds numbers, the gap is not completely gasproof. The gas in the gap has two major consequences: (i) it partially sustains the outer disc, effectively reducing the torque felt by the planet from the outer disc; (ii) it exerts a corotation torque on to the planet. The possibility of gas flowing through the gap decouples the planet from the gas evolution.

In this section we show with a simple model that taking into account these effects allows us to explain the evolution of the planet as a function of the various parameters. Our model is based on previous works on the corotation torque (Masset 2001), the viscous evolution of accretion discs (LP74) and the shape of gaps (Crida et al. 2006).

6.1 Classical type II torque

In an accretion disc, the viscous stress is such that angular momentum flows outward while matter falls on to the star. In a Keplerian, circular disc with ν and Σ independent of the radius, the torque exerted by the part of the disc extending from a given radius r_0 to infinity on the inner part $\{r < r_0\}$ is $T_\nu = -3\pi\Sigma\nu {r_0}^2\Omega_0$ (it can be easily found from the strain tensor). It causes a mass flow of gas F, carrying the equivalent angular momentum: $T_\nu = F{r_0}^2\Omega_0 = (2\pi r_0\Sigma v_\mathrm{r})\, {r_0}^2\Omega_0$, where v_r is the radial velocity of the gas. In this model $v_\mathrm{r} = -(3/2)(\nu/r_0)$, which can also be found from the Navier–Stokes equations. This gives the following equality, which we will use further:

$$\nu = -\frac{2v_\mathrm{r}}{3} r_0. \tag{5}$$

If a planet opens a deep gap in such a disc, no gas flow is allowed through the planetary orbit. The outer disc is maintained outside of the gap by the planet, and an equilibrium is reached so that the planetary torque balances T_ν. Consequently, the planet feels from the outer disc the torque T_ν. This torque is proportional to the viscosity and not to the planet mass. This is the case of standard type II migration.

In a more realistic, viscously evolving disc, the scheme for type II migration is the same, but the above formula for T_ν is no longer valid. In that case, the equations of LP74 provide the density, the viscous torque and the radial velocity as a function of radius and time. In our case of a disc with $R_\mathrm{inf} > 0$, it gives

$$T_\nu = 3\pi\nu\Sigma_0 T^{-5/4}\,(h - h_\mathrm{inf}) \exp\left(-\frac{ar^2}{T}\right), \tag{6}$$

$$\Sigma_\mathrm{LP74} = \frac{T_\nu}{3\pi\nu\sqrt{r}}, \tag{7}$$

$$F = -\frac{\partial T_\nu}{\partial h}, \tag{8}$$

$$v_\mathrm{r} = \frac{F}{2\pi r\,\Sigma_\mathrm{LP74}}, \tag{9}$$

where $h = r^2\Omega = \sqrt{r}$ is the specific angular momentum. Notice that equation (6) is exactly equation (25) in LP74, while equation (7) is equivalent to equation (2).

Thus, in standard type II migration, we consider that the planet feels from the disc a torque

$$T_\mathrm{II} = Fh = 2\pi {r^+}\Sigma_\mathrm{LP74}(r^+) v_\mathrm{r}(r^+)\sqrt{r^+}, \tag{10}$$

where $r^+ = r_\mathrm{p} + x_\mathrm{s}$ is the radius of the external edge of the gap, and Σ_LP74 and v_r come from equations (7) and (9), respectively.

6.2 Torque exerted on the outer disc by the gas in the gap

The gas in the gap, the density of which is denoted Σ_gap, exerts on the outer disc a positive viscous torque $T_{(i)}$ that is given by equation (10), with Σ_gap instead of Σ_LP74 and the opposite sign. This torque partially sustains the outer disc, and therefore needs to be subtracted from the torque that the planet would suffer from the outer disc if the gap were clean (given by equation 10). So, denoting by f the ratio $\Sigma_\mathrm{gap}/\Sigma_\mathrm{LP74}$ we have

$$T_{(i)} = -f T_\mathrm{II}. \tag{11}$$

We now discuss how to evaluate f in practice. We have presented in Section 5 a way to compute semi-analytically the gap profile and the gap depth. However, making a step-by-step integration until the bottom of the gap it is not very convenient. Consequently, we looked for a simple empirical formula for the gap depth as a function of the viscosity, the aspect ratio of the disc and the planet mass. Crida et al. (2006) showed that the density inside the gap is less than 10 per cent of the unperturbed value (i.e. $f < 0.1$) if and only if

$$\mathcal{P} = \frac{3}{4}\frac{H}{R_\mathrm{H}} + \frac{50}{q\mathcal{R}} \lesssim 1. \tag{12}$$

Using equation (3), we have computed the depth of the gap for various values of the parameter $\mathcal{P}$. For each value of $\mathcal{P}$, we impose $q = 10^{-3}$ and $H/r = 0.05$, and find the corresponding viscosity. Then, we use these parameters in equation (3); the obtained gap depth is shown as big dots in Fig. 8. We repeat the same operation for q ranging from 5×10^{-4} to 2×10^{-3}; the results are reported as crosses in Fig. 8. Furthermore, we impose $q = 10^{-3}$ and $\nu = 0$, and find the corresponding H/r and the resulting gap depth. We

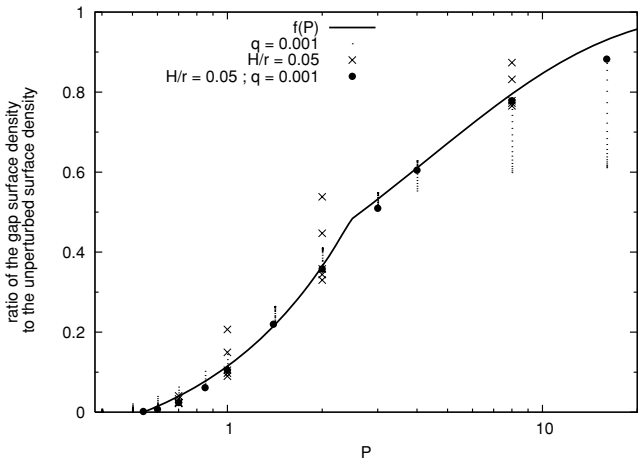

Figure 8. Gap depth (measured as ratio of the gap surface density to the unperturbed density at $r = r_\mathrm{p} + 2R_\mathrm{H}$) as a function of $\mathcal{P}$. The data points for each value of $\mathcal{P}$ are obtained from the integration of equation (3), assuming different values of ν and H/r and keeping $q = 10^{-3}$ (points) or different values of ν and q and keeping $H/r = 0.05$ (crosses); the big dots correspond to the gap depths obtained for different values of ν and keeping both $H/r = 0.05$ and $q = 10^{-3}$ (see text for a more precise description of the sets of measures). The bold line is an approximate fit of the data.

repeat the operation for ν ranging up to its maximum possible value compatible with $\mathcal{P}$; the results are shown as dots in Fig. 8. Finally, for a given value of $\mathcal{P}$, different depths are observed because the shape of the gap is not the same whether the viscosity or the pressure dominates. However, there is a very clear tendency for deeper gaps with decreasing $\mathcal{P}$, as could be expected. The bold line in Fig. 8 shows the fit that we adopt:

$$f(\mathcal{P}) = \begin{cases} (\mathcal{P} - 0.541)/4 & \text{if } \mathcal{P} < 2.4646, \\ 1 - \exp[-(\mathcal{P}^{0.75}/3)] & \text{if } \mathcal{P} \geqslant 2.4646, \end{cases} \quad (13)$$

where $f(\mathcal{P})$ stands for $\Sigma_{\rm gap}/\Sigma_{\rm LP74}$.

As the gap depth given by equation (3) is not very precise and shows variations at fixed $\mathcal{P}$, this fit is clearly a crude approximation of the real depth. However, the evolution of the gap depth as a function of the parameters is satisfactorily described by $f(\mathcal{P})$, in particular if one imposes $q = 10^{-3}$ and $H/r = 0.05$, which is the most common case for us. As we are looking for a simple model, this approximation is sufficient for our purpose.

6.3 Corotation torque

In Masset (2001), the corotation torque is computed as

$$T_{\rm C} = \frac{3}{2}{\Omega_{\rm p}}^2 {x_{\rm s}}^4 \Sigma_\infty \mathcal{F}(z_{\rm s}),$$

where Σ_∞ is the unperturbed surface density (assumed to be independent of radius), $z_{\rm s} = (\mathcal{R}/2\pi)^{1/3} x_{\rm s}/r_{\rm p}$, the function $\mathcal{F}(z) = z^{-3} - z^{-4} g(z)/g'(z)$ and g is a linear combination of the Airy functions Ai and Bi defined in equation (A18) of Masset (2001). This formula can easily be generalized for an arbitrary profile of Σ (see Ward 1991), and be rewritten as

$$T_{\rm C} = \frac{3}{4}{\Omega_{\rm p}}^2 {x_{\rm s}}^4 \Sigma \frac{{\rm d}\log(\Sigma/B)}{{\rm d}\log r} \hat{\mathcal{F}}\left(\frac{1}{(x_{\rm s}/r_{\rm p})^3 \mathcal{R}}\right),$$

where B is the second Oort constant ($B = \Omega/4$ in Keplerian rotation), and $\hat{\mathcal{F}}(z) = 4\mathcal{F}[(z/2\pi)^{(1/3)}]$.

The function $\hat{\mathcal{F}}(z)$ is shown in graphical form in fig. 2 of Masset (2001). For $z < 0.1$ (which is our case if we consider $x_{\rm s} = 2R_{\rm H}$, $q = 10^{-3}$ and $\mathcal{R} > 10^{3.6}$) one has $\hat{\mathcal{F}}(z) \approx 20z$. Thus, we may write

$$T_{\rm C} = \frac{3}{4} 20 x_{\rm s} \Omega_{\rm p} {r_{\rm p}}^2 \Sigma \nu \frac{{\rm d}\log(\Sigma/B)}{{\rm d}\log r}.$$

In Masset (2001), the approximation that ν and Σ are independent on r is made. Thus, we can use equation (5) and write equivalently

$$T_{\rm C} = -10\, x_{\rm s} \Omega_{\rm p} {r_{\rm p}}^2 \Sigma v_{\rm r} \frac{{\rm d}\log(\Sigma/B)}{{\rm d}\log r}. \quad (14)$$

Here, Σ is the density inside the gap, which is equal to $\Sigma_{\rm LP74}(r^+) f(\mathcal{P})$, and $v_{\rm r}$ is the radial velocity at $r = r_{\rm p}$, which is given in equation (9). The term $({\rm d}\log(\Sigma/B))/({\rm d}\log r)$ is computed from the unperturbed density $\Sigma_{\rm LP74}(r)$, assuming a Keplerian rotation of the disc.

6.4 Total torque exerted on the planet

The total torque felt by the planet is, therefore, $T_{\rm p} = T_{\rm II} - T_{(i)} + T_{\rm C}$. From equations (10), (11) and (14), the total torque reads

$$T_{\rm p} = 2\pi r^+ \Sigma_{\rm LP74}(r^+) v_{\rm r}(r^+) \sqrt{r^+} \times \left[1 - f(\mathcal{P}) - \frac{15}{2\pi} \frac{x_{\rm s}}{r^+} \frac{\Omega_{\rm p} {r_{\rm p}}^2}{\sqrt{r^+}} \frac{v_{\rm r}(r_{\rm p})}{v_{\rm r}(r^+)} f(\mathcal{P}) \frac{{\rm d}\log(\Sigma/B)}{{\rm d}\log r}\right], \quad (15)$$

with $\mathcal{P}$ and f defined, respectively, in equations (12) and (13), while $r^+ = r_{\rm p} + x_{\rm s}$, $x_{\rm s} = 2R_{\rm H}$ and $\Sigma_{\rm LP74}$ and $v_{\rm r}$ come from equations (6)–(9). This expression involves (directly or via $v_{\rm r}$ or $\Sigma_{\rm LP74}$) the viscosity of the disc ν, its aspect ratio H/r, the planet to primary mass ratio q, the radius of the planetary orbit $r_{\rm p}$ and the radius of the inner edge of the disc $R_{\rm inf}$. In the following, we test it against numerical simulations for a wide range of these parameters.

6.4.1 Dependence on the Reynolds number

In the top panel of Fig. 9 we plot the total torque felt by a Jupiter mass planet located at $r_{\rm p} = 5$ au in a disc with 0.05 aspect ratio and $R_{\rm inf} = 0.65$ au as a function of $\mathcal{R}$. The torque given by equation (15) with $t = t_\nu/100$ is plotted as a bold line. The crosses with the error bars represent the torque felt by the planet in the numerical simulation, measured at $t = t_\nu/100$ (so that the planet is still at about $r_{\rm p} = 5$ au). The error bars correspond to the maximum and minimum migration rates measured between $t_\nu/200$ and $t_\nu/50$. The torque $T_{\rm II}$, corresponding to classical type II migration, is drawn as a thin line; it is proportional to $\nu \propto \mathcal{R}^{-1}$. The bottom panel shows, as reference, the gap depth $f(\mathcal{P})$ as a function of $\mathcal{R}$.

As one can see in Fig. 9, the model reproduces very well the general tendency. For $\mathcal{R} > 10^5$, $f(\mathcal{P}) < 0.125$ and $T_{\rm p}$ is close to $T_{\rm II}$, negative and proportional to the viscosity, as expected in proper type II migration; in other words, $T_{\rm II}$ dominates $T_{(i)}$ and $T_{\rm C}$ in the calculation of $T_{\rm p}$. For lower Reynolds numbers, the effects of the gas in the gap counterbalance the classical $T_{\rm II}$. For $\mathcal{R} < 10^4$, $f(\mathcal{P}) > 0.7$ and the total torque is positive. Both the measures from the simulations and the results of equation (15) show a minimum of the torque felt by the planet at about $\mathcal{R} = 10^{4.5}$. This shows that type II migration speed is bounded. One could think that an increase in the gas viscosity, and therefore of the gas accretion rate, would

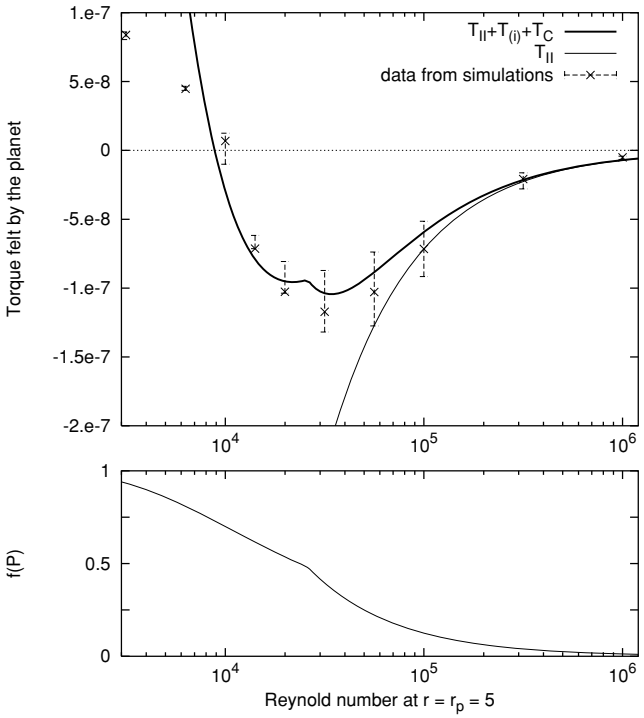

Figure 9. Top panel: torque felt by the planet, expressed in the units defined in Section 3.2, as a function of the Reynolds number. Bottom panel: the gap depth $f(\mathcal{P})$ as a function of the same parameter.

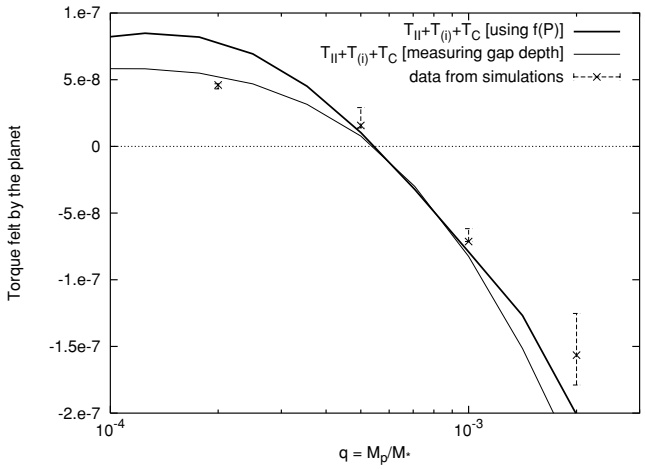

Figure 10. Torque felt by a planet as a function of its mass.

increase the type II migration speed of a giant planet. In reality, this favours the filling of the gap, which decouples the planet from the disc evolution.

Notice however that for very low Reynolds number (high viscosity) our model reaches its validity limits. In fact, our model predicts a very fast outward migration, which is not observed in the simulations. In these cases, $f(\mathcal{P})$ is more than 0.8 (essentially no gap), so that the basic idea on which our model is built is no longer valid. Eventually, for large enough viscosity, the planet has to migrate inward, at a type I migration rate.

6.4.2 *Dependence on the planet mass*

In Fig. 10, the torque exerted on a planet placed at $r_p = 5$ in a disc with $\mathcal{R} = 10^{4.15}$, $H/r = 0.05$ and $R_{inf} = 0.65$ is plotted as a function of the planet mass. The bold line corresponds to our model, and the crosses correspond to numerical experiments (with the error bars computed with the same prescription as before). Once again, we recover the observed trend. The discrepancy at very low mass comes in fact from the estimation of the gap depth $f(P)$; for $q < 5 \times 10^{-4}$, the density in the 'gap' is larger than 0.8, so that the gap is shallow and f is not very accurate. Using directly equation (3) instead of prescription equation (13) for the gap depth gives a better result, shown as a thin line; this validates again our model.

The torque felt by the planet is a decreasing function of its mass. The explanation for this behaviour is quite easy: the lighter is the planet the shallower is the gap, and the more important are the effects of the gas in the gap on the total torque. Symmetrically, the more massive is the planet the deeper is the gap it opens, and thus the closer to type II migration is its migration regime.

This result is relevant for extrasolar planets as it can explain why, of the many couples of resonant planets, typically the most massive object is the outermost one. Indeed, resonant capture is possible only if the outer planet migrates inward faster than the inner planet which, according to Fig. 10, requires that the outer planet is the most massive.

6.4.3 *Dependence on planet accretion*

The planet mass is not necessarily constant. Planets are supposed to accrete gas continuously. Gas accretion by the planet perturbs the gas flow through the planetary orbit; in addition, mass accretion

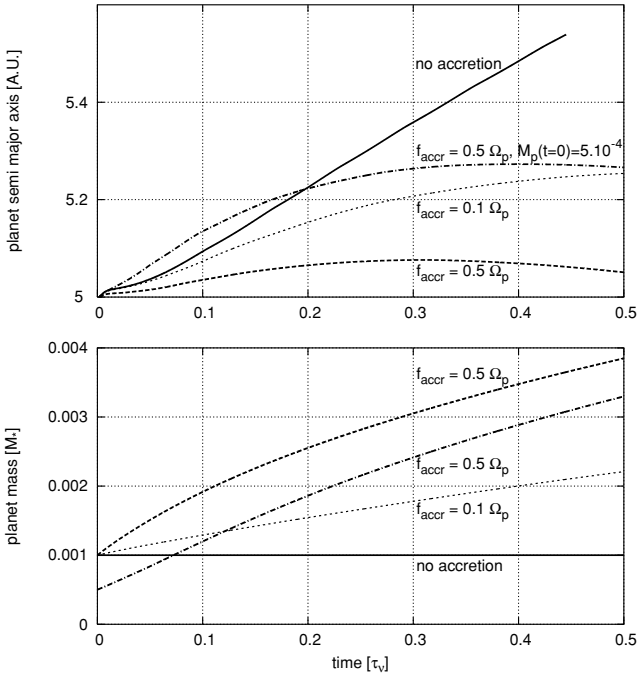

Figure 11. Top panel: migration of accreting giant planets in a disc with $\mathcal{R} = 10^{3.8}$ and $H/r = 0.05$. Bottom panel: corresponding evolution of their masses.

exerts an additional torque on the planet (Lubow & D'Angelo 2006). Therefore, in principle, accretion could change the dynamics. We have implemented planetary accretion following the recipe of Kley (1999): it consists in removing a fraction of the material in the Hill sphere of the planet and adding it to the mass of the planet. The accretion rate, expressed as a fraction of mass removed per time unit is imposed as an input parameter. More precisely, we apply the input removal rate f_{accr} in the inner part of the Hill sphere (extended up to $0.45\,R_H$), and two thirds of f_{accr} in the region from $0.45R_H$ to $0.75R_H$.

Considering $\mathcal{R} = 10^{3.8}$ and $H/r = 0.05$, we performed simulations of a Jupiter mass planet initially on a circular orbit at 5 au, with input removal rates $f_{accr} = 0.5\Omega_p$ and $f_{accr} = 0.1\Omega_p$. The results in terms of migration and accretion are shown in Fig. 11 and compared with the no accretion case. Another simulation with input removal rate $0.5\Omega_p$ and initial mass of the planet 5×10^{-4} is also performed. The results show that accretion does not prevent outwards migration. The comparison between the top panel (migration) and the bottom panel (mass evolution) shows that the migration speed seems to be governed by the planet mass, and not by the accretion rate. While the accretion rate is constant with time in all cases, the migration rate is not, and its evolution follows the evolution of the planet mass. As expected from the discussion above, the outwards migration rate is slower for more massive planets; if the planet reaches 3 Jupiter masses, its migration vanishes; the migration is directed inwards for more massive planets.

6.4.4 *Dependence on the radii of the planetary orbit and of the disc inner edge*

One may wonder about the dependence of the migration rate on the planet's location in the disc. This is governed by the radial dependence of viscosity and aspect ratio.

If the viscosity is constant, the Reynolds number $\mathcal{R}$ increases as $\sqrt{r}$. Thus, the depth of the gap opened by the planet *increases* with the planet's location r_p. As a consequence a planet should migrate inward if it is sufficiently far from the star, and outward if it is sufficiently close. The migration paths therefore converge towards the stationary solution, at some specific radius, dependent on viscosity and planet mass.

However, if the viscosity of the disc depends on radius as described in an α model (Shakura & Sunyaev 1973), the Reynolds number is independent of radius. If the disc is flared, H/r increases with r and therefore the depth of a gap opened by the planet *decreases* with r_p. Consequently, the planet tends to move outward if it is far from the star and inward if it is close. Any stationary solution would therefore be unstable.

If the disc is not flared and the Reynolds number does not depend on r, then the behaviour of the planet depends on the ratio r_p/R_{inf}. This effect is subtle. If the ratio r_p/R_{inf} is smaller, the planet is in a location of the disc where Σ and v_r have a steeper positive slope, and v_r is also larger in absolute value, following equation (9). In our model, the gas radial velocity multiplies all the torques that appear in equation (15). Therefore, the only dependence on r_p/R_{inf} is through the gradient of the gas radial velocity $v_r(r_p)/v_r(r^+)$ and the gradient of the logarithm of the density that appear in equation (15) for the corotation torque. Fig. 12 shows as a bold line the torque felt by a Jupiter mass planet for $\mathcal{R} = 10^{4.15}$ at $t = t_\nu/100$, as expected in our model. The gradient effect becomes important when $R_{inf}/r_p \geqslant 1/2$. The crosses with the error bars correspond to measures from numerical simulations. Once again, our model reproduces very well the observed trend.

This result might be relevant to explain the existence of hot or warm Jupiters. Although several solutions have been proposed, the issue of why these planets did not migrate all the way into their parent stars remains open. Fig. 12 shows that, for the parameters used in that calculation, a planet approaching the inner edge of the disc has eventually to stop at the location where the migration rate turns from negative to positive. Therefore, the survival of some hot/warm Jupiters against migration seems to be a natural consequence of the local surface density gradient at the inner edge of the disc, predicted by LP74. Notice however that some hot Jupiters are so close to the central star that they are presumably well within the corotation radius. As the disc inner edge should not have been closer than the corotation radius, these planets somehow managed to migrate past the inner edge of the disc. In the framework of our model this may be possible for massive planets in low-viscosity discs, opening deep and clean gaps. In these cases, the planets presumably stopped migrating when their outer 1:2 mean motion resonances reached the inner disc edge, as proposed in Kuchner & Lecar (2002). In conclusion, the dynamical diversity of the exoplanets could be a consequence of the physical diversity of the protoplanetary discs.

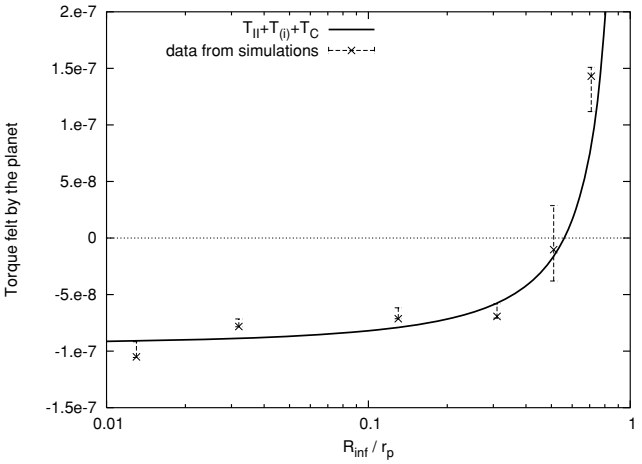

Figure 12. Torque felt by a Jupiter mass planet at $r_p = 5$ with $\mathcal{R} = 10^{4.15}$, $H/r = 0.05$, at $t = t_\nu/100$, as a function of the radius of the inner edge of the disc R_{inf}.

7 EFFECT OF PLANET MIGRATION ON THE INNER DISC DEPLETION

In Fig. 6 we have shown that in the case of a non-migrating planet, the density profile in the inner part of the disc coincides with the unperturbed profile given by LP74 equations. This showed that the overall mass flow through the disc was unperturbed by the presence of the planet.

Fig. 13 is the same as Fig. 6 but for a case where the planet moves inward at slow rate. In this case there appears to be a deficit in the inner part of the disc, while the outer part shows a little overdensity, relative to the unperturbed case and to the prediction of our simple model. This reveals that only a fraction of the unperturbed mass flow effectively passes from the outer to the inner disc.

Based on the model developed above, we can illustrate this fact and develop an a priori estimate of the inner disc mass deficit.

Because of the migration of the planet, the surface of the inner disc shrinks at a speed

$$\dot{A}_p = 2\pi r_p \dot{r_p}.$$

In the unperturbed case, if we draw a fictitious boundary between the inner and the outer disc moving at the radial velocity of the gas, the surface of the inner disc shrinks at a speed

$$\dot{A}_{unp} = 2\pi r_p v_r.$$

Thus, for the inner mass of the disc to remain the same as in the unperturbed case, the mass flow into the inner disc through a planet's gap must be equal to

$$\dot{M}_0 = -(\dot{A}_{unp} - \dot{A}_p)\Sigma = 2\pi r_p(\dot{r_p} - v_r)\Sigma,$$

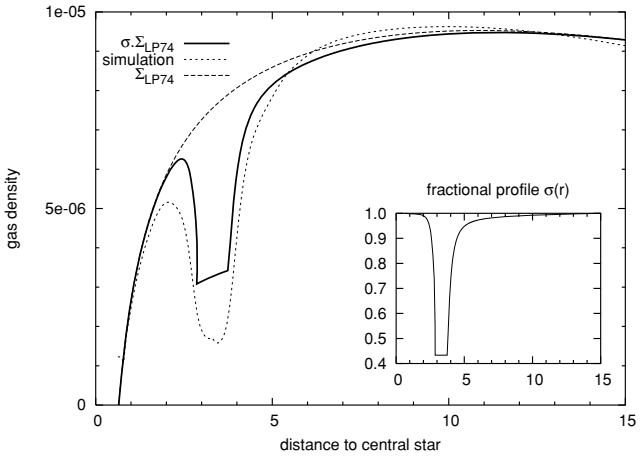

Figure 13. Gap profile in an evolving disc with $\mathcal{R} = 10^{4.5}$: the thin, short-dashed line results from numerical simulation while the bold, plain line comes from our simple model. Long-dashed line: the unperturbed profile $\Sigma_{LP74}(r, t_\nu/2)$ from equation (2). Secondary panel: 'fraction profile' $\sigma(r)$ of the gap integrated from equation (14) of Crida et al. (2006).

where Σ is the unperturbed gas density, to be identified with $\Sigma_{\rm LP74}$ above. The mass flow into the inner disc through the planet's gap corresponds to the angular momentum loss of the outer disc. It can be expressed as

$$\dot{M}' = -\dot{J}_{\rm o}/j, \tag{16}$$

where $J_{\rm o}$ is the total angular momentum of the outer disc and j is the specific angular momentum. Obviously, $\dot{J}_{\rm o} = \dot{J}_{\rm o,unp} - \dot{J}_{\rm p}$, where $\dot{J}_{\rm o,unp}$ is the change of angular momentum of the outer disc in the unperturbed case and $\dot{J}_{\rm p}$ is the change of angular momentum of the planet.

Thus, the mass flow deficit into the inner disc is

$$\delta\dot{M} = \dot{M}_0 - \dot{M}' = 2\pi r_{\rm p}(\dot{r_{\rm p}} - v_{\rm r})\Sigma + (\dot{J_{\rm o,unp}} - \dot{J}_{\rm p})/j. \tag{17}$$

Now, remembering that $\dot{J}_{\rm p} = \dot{r_{\rm p}} M_{\rm p}/2\sqrt{r_{\rm p}}$ and that $\dot{J}_{\rm o,unp} = 2\pi r_{\rm p} v_{\rm r} \Sigma j$, the expression above becomes

$$\delta\dot{M} = \frac{\dot{J}_{\rm p}}{j}\left(4\frac{\mu}{q} - 1\right), \tag{18}$$

where $\mu = \pi r_{\rm p}^2 \Sigma / M_*$ and $q = M_{\rm p}/M_*$ are the reduced masses of the inner disc and the planet.

Some remarks on equation (18) are in order. If the planet does not migrate, $\dot{J}_{\rm p} = 0$ and thus there is no mass flow deficit into the inner disc, in agreement with Fig. 6. If $q = 4\mu$ there is also no mass deficit in the inner disc. This case corresponds to $\dot{r_{\rm p}} = v_{\rm r}$, that is to a planet that migrates inward at the same speed of the unperturbed gas. We recall that this is the maximal migration speed of a planet in type II migration. So, if $q < 4\mu$, equation (18) does not apply.

Finally, to compute the mass of the inner part of the disc (and therefore the cavity depth) one can follow the approach illustrated in Section 5 and multiply the result by

$$1 - \delta\dot{M}/\dot{M}_0 = 1 - \frac{q/4\mu - 1}{(q/4\mu)(\dot{J_{\rm o,unp}}/\dot{J}_{\rm p}) - 1}. \tag{19}$$

From equation (19), it also appears that if the planet mass is large with respect to the disc mass, then the mass flow deficit $\delta\dot{M}/\dot{M}_0$ tends to $\dot{J}_{\rm p}/\dot{J}_{\rm o,unp}$. If this planet opens a clean gap, $\dot{J}_{\rm p} \approx \dot{J}_{\rm o,unp}$ and $\dot{r_{\rm p}}/v_{\rm r} \ll 1$, so that $\delta\dot{M} \approx \dot{M}_0$. In summary, the two conditions $q/\mu \gg 1$ and formation of a clean gap are required to deplete strongly the inner disc and form a deep cavity.

To confirm this result, we performed a simulation with the same Jupiter mass planet initially placed on a circular orbit at $r_{\rm p} = 5$ au, and the same initial disc profile as before, except that the gas density is divided by 100. The Reynolds number is taken equal to 10^5 and the aspect ratio is decreased to 0.03 for the planet to open a cleaner gap than before. Fig. 14 displays the resulting disc profile at $t = t_\nu/2$ (thin solid curve): one can see that the planet did almost not migrate, but the inner disc has been significantly depleted with respect to the unperturbed profile (thin dotted curve) and to the profile given by equation (4) (bold solid curve). As we have seen above, for 'reasonable' values of disc height and viscosity a Jupiter mass planet does not open a very clean gap. So, in practice, an effective cavity opening planet would need to have 3–5 Jupiter masses, embedded in a sub-Jovian mass disc.

The migration rate of the planet at $t = t_\nu/2$ in the simulation is $\dot{J}_{\rm p} = 2.88\times10^{-11}$. The unperturbed density is $8.48 \times 10^{-8}\,{\rm M}_\odot\,{\rm au}^{-2}$ so that $q/4\mu = 36.84$, and the unperturbed radial velocity of the gas is -1.03×10^{-5}. Following equation (19), this gives a relative mass deficit in the inner disc:

$$\delta\dot{M}/\dot{M}_0 = 0.45.$$

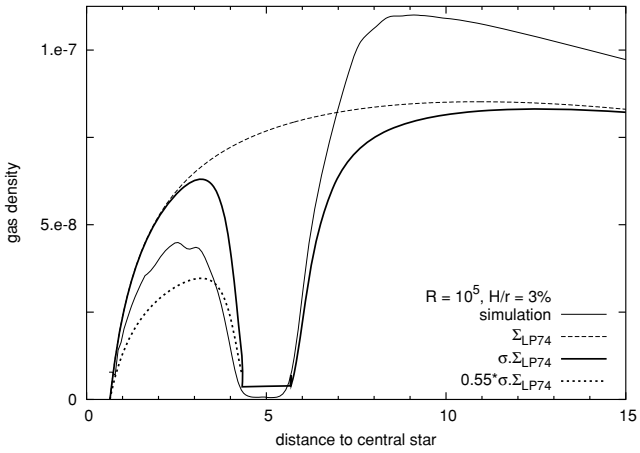

Figure 14. Gap profile in a small mass evolving disc with $\mathcal{R} = 10^5$ and $H/r = 0.03$: the thin solid curve results from a numerical simulation while the bold line comes from our simple model. Thin dashed curve: the unperturbed profile $\Sigma_{\rm LP74}(r, t_\nu/2)$ from equation (2). Bold dotted curve: the inner disc profile in our model, multiplied by the estimated relative mass deficit.

Our model density profile, multiplied by 0.55 gives for the inner disc the bold dotted curve in Fig. 14. This agreement is quite satisfactory, although – admittedly – a better agreement with the real inner disc profile would be given by a coefficient of about 0.75.

8 GAS CAVITIES VERSUS DUST CAVITIES

Up to this point, we have discussed only the gas distribution of the disc. However, the observations reviewed in Section 2 constrain the absence of dust in the inner part of the disc, rather than the absence of gas.

The dust distribution and the gas distribution are not necessarily the same. As recently pointed out by Rice et al. (2006) (see also Paardekooper & Mellema 2006), the opening of a gap in the gas disc can act as a filter on the dust. Only the very small dust can flow with the gas through the gap and refill the inner part of the disc. Larger dust particles are repelled by the positive gas pressure gradient at the outer edge of the gap, and consequently they cannot pass through the planet's orbit.

Our model provides all the ingredients to compute what is the maximal size of dust particles that can flow with the gas through the gap as a function of the various parameters of the problem (planet mass, $\mathcal{P}$ etc.), as outlined below.

The gas orbital velocity $v_{\rm g}$ differs from the Keplerian velocity $v_{\rm K}$ due to pressure effects as

$$\frac{v_{\rm g}^2}{r} = \frac{v_{\rm K}^2}{r} + \frac{1}{\Sigma}\frac{{\rm d}P}{{\rm d}r},$$

where P is the pressure and Σ is the surface density. Using our equation of state (see Section 3.2) and assuming that sound speed $c_{\rm s}$ does not change significantly along the gap's edge, the last term of the above equation can be rewritten as $(1/\Sigma)\,{\rm d}\Sigma/{\rm d}r$. Its maximum value can be obtained from equation (3) at $r = r_{\rm p} + 2R_{\rm H}$.

Once $v_{\rm g}$ is computed, the outward drift speed $v_{\rm r}^{\rm (d)}$ of a dust particle of a given size and density can be computed following Weidenschilling (1977). The quantity $v_{\rm r}^{\rm (d)}$ is actually a speed relative to the gas radial motion. Thus, if the inward radial velocity of the gas $v_{\rm r}^{\rm (g)}$ is larger in absolute value than $v_{\rm r}^{\rm (d)}$, the dust flows inwards, passing through the planet's gap. In the opposite case the dust is repelled by the pressure gradient and accumulates at the edge

of the gap. The radial velocity of the gas at the base of the gap, where the pressure effect on the dust is maximal, can be computed as

$$v_{\rm r}^{\rm (g)} = \frac{\dot{M}'}{2\pi r_{\rm p} \Sigma f(\mathcal{P})}, \tag{20}$$

where $\dot{M}'$ is given in equation (16). Assuming that the mass flux from the outer to the inner disc is not strongly perturbed by the presence of the planet (i.e. $\dot{M}' \sim \dot{M}_0$, which is strictly true in the case of a non-migrating planet) one has

$$v_{\rm r}^{\rm (g)} = \frac{v_{\rm r}}{f(\mathcal{P})}, \tag{21}$$

where $v_{\rm r}$ is given in equation (9). Finally, because $v_{\rm r}^{\rm (d)}$ depends on the dust particle size, the equation $|v_{\rm r}^{\rm (d)}| = |v_{\rm r}^{\rm (g)}|$ gives the maximal size of the particles that flow in the inner disc with the gas.

However, we think that it is not evident that a real dust cavity is opened inside the orbit of the planet, even for dust sizes that cannot pass through the gap. The dust in the inner disc should accumulate at the place of the relative maximum of the gas density distribution, rather than follow the gas in its accretional motion on to the star. In fact, the positive density gradient at the inner edge of the disc is comparable to that at the outer edge of the gap opened by the planet (see Figs 1 and 7). So, if the dust is repelled by the gap edge, it should also be repelled by the inner disc edge. In this situation a ring of dust should form in the inner disc, its width depending on the local velocity dispersion due to the turbulence. Hence, the planet appears opening a wide and deep gap in the dust distribution (Paardekooper & Mellema 2006), rather than a cavity. This, however, may still be consistent with the observations: if these rings of large dust grains are very narrow (as they may well be) the particles may not contribute significantly to the observed SED; so, the SED observations would still suggest an inner cavity with small grains (producing a 10-μm feature) and a population extending to larger sizes in the outer disc.

Possibilities to get rid of the larger dust grains in the inner disc could be (i) the collisional comminution into smaller particles that are coupled to the gas and therefore – as the gas – accrete on to the star, (ii) formation of larger particles or planetesimals favoured by the high dust density in the ring and (iii) sublimation of the dust if the ring is located sufficiently close to the star. Obviously the situation is complicated. The study of the dust distribution requires the use of an adapted bifluid code, including irradiation effects. This should be the object of future work.

9 CONCLUSION

In this paper, we have performed numerical simulations of giant planets embedded in a gas disc of equivalent mass. The disc in the simulations is viscously evolving, reproducing (in absence of planetary perturbation) the evolution described in LP74. This is made possible by the use of a new numerical scheme that complements the usual 2D grid with a 1D grid spanning over the assumed physical extension of the disc (Crida et al. 2007), so that the global evolution of the disc is taken into account. This is a key point for the accurate simulation of both the cavity opening process and the planet migration. Indeed, the first phenomenon depends on the accretion of the inner disc on to the central star; thus the simulation of the disc evolution down to its physical inner edge is necessary for reliable results. As for the planetary migration, proper type II migration corresponds to the case where the planet follows the disc evolution; the global evolution of the disc is thus the key phenomenon that needs to be reproduced.

If the disc mass is not negligible with respect to the planet mass, we found that the planet does not modify substantially the disc profile with respect to the free viscous evolution; it simply opens a more or less deep gap in the unperturbed profile. Consequently, the opening of a cavity mainly depends on the position of the planetary orbit with respect to the inner edge of the disc $R_{\rm inf}$. Indeed, at this inner edge, the density is 0. It grows with r until the inner edge of the gap. Thus, if the gap is close to the inner edge of the disc, the density in the inner disc does not reach the maximum value and a cavity appears. As a result, it is much easier to open cavities in discs with large $R_{\rm inf}$ than in discs with small $R_{\rm inf}$. The size of this inner radius may vary in astrophysical discs, depending on the process that governs the fall of the gas on to the central star. We stress that one should be aware of the primordial influence of this parameter on the inner disc evolution when computing numerical simulations.

In the intermediate regime between type I and type II migration – where the planet opens a non-gasproof gap – the migration may be stopped or reversed. In fact, if the gap is not clean, the gas in the gap exerts a positive viscous torque on the outer disc, so that the outer disc does not push the planet inward as efficiently as when the gap is clear. In addition, the corotation torque is positive and proportional to the density in the corotating zone. Thus, the total torque felt by the planet may be zero, or even positive, if the Reynolds number is low enough (Fig. 9). We built a model based on simple, qualitative ideas that leads to a simple expression of the total torque felt by a planet in an evolving disc (equation 15). This enabled us to reproduce the dependence of planet migration on the various parameters. Viscosity plays a major role: standard type II migration occurs only when the planet opens a very clean gap, that is at low viscosity; if the viscosity increases, the gap becomes less depleted and less gasproof, which leads to the decoupling of the migration with respect to the disc evolution. The role of the planet mass is very intuitive: the more massive is the planet the deeper is its gap and thus the closer to standard type II migration is its behaviour. Last, the role of the radius of inner edge of the disc $R_{\rm inf}$ is significant only when it is more than about half the orbital radius of the planet: in that case, the density gradient of the disc at the planet location increases with $R_{\rm inf}$, which enhances the corotation torque and makes the planet migrate outward.

In conclusion, under some conditions on the disc parameters, type II migration may be avoided for a Jupiter mass planet at 5 au in an accreting disc, provided it does not open a very deep gap. This could explain why all the known giant planets (in the Solar system and in extra-Solar systems) are not hot Jupiters. Our results also explain why hot Jupiters had to stop migrating before falling on to their parent stars. They also explain why, among pairs of resonant planets, the outermost one is typically the most massive object.

ACKNOWLEDGMENTS

We wish to thank W. Kley, F. Masset, R. P. Nelson and A. Quillen for discussions and suggestions. We are grateful to the French National Programme of Planetary Science (PNP) for financial support. We also wish to thank the anonymous reviewer for interesting suggestions on the hot and warm Jupiters and the dust dynamics.

REFERENCES

Bacciotti F., Ray T. P., Eislöffel J., Woitas J., Solf J., Mundt R., Davis C. J., 2003, Ap&SS, 287, 3

Beckwith S. V. W., 1999, in Lada C. J., Kylafis N. D., eds, NATO ASIC Proc. 540, The Origin of Stars and Planetary Systems. Kluwer, Dordrecht, p. 579

Bergin E. et al., 2004, ApJ, 614, L133
Bodenheimer P., Hubickyj O., Lissauer J. J., 2000, Icarus, 143, 2
Calvet N., D'Alessio P., Hartmann L., Wilner D., Walsh A., Sitko M., 2002, ApJ, 568, 1008
Calvet N. et al., 2005, ApJ, 630, L185
Coffey D., Bacciotti F., Woitas J., Ray T. P., Eislöffel J., 2004, ApJ, 604, 758
Crida A., Morbidelli A., Masset F., 2006, Icarus, 181, 587
Crida A., Morbidelli A., Masset F., 2007, A&A, 461, 1173
Dullemond C. P., Dominik C., Natta A., 2001, ApJ, 560, 957
Forrest W. J. et al., 2004, ApJS, 154, 443
Goldreich P., Tremaine S., 1979, ApJ, 233, 857
Guillot T., Hueso R., 2006, MNRAS, 367, L47
Hayashi C., 1981, Prog. Theor. Phys. Suppl., 70, 35
Kley W., 1999, MNRAS, 303, 696
Kuchner M. J., Lecar M., 2002, ApJ, 574, L87
Lin D. N. C., Papaloizou J., 1979, MNRAS, 186, 799
Lubow S. H., D'Angelo G., 2006, ApJ, 641, 526
Lynden-Bell D., Pringle J. E., 1974, MNRAS, 168, 603 (LP74)
Masset F., 2000a, A&AS, 141, 165
Masset F., 2000b, in Garzón G., Eiroa C., de Winter D., Mahoney T. J., eds, ASP Conf. Ser. Vol. 219, Disks, Planetesimals, and Planets. Astron. Soc. Pac., San Francisco, p. 75
Masset F. S., 2001, ApJ, 558, 453
Mayor M., Queloz D., 1995, Nat, 378, 355
Paardekooper S.-J., Mellema G., 2006, A&A, 453, 1129
Piétu V., Dutrey A., Guilloteau S., Chapillon E., Pety J., 2006, A&A, 460, L43
Pollack J. B., Hubickyj O., Bodenheimer P., Lissauer J. J., Podolak M., Greenzweig Y., 1996, Icarus, 124, 62
Quillen A. C., Blackman E. G., Frank A., Varnière P., 2004, ApJ, 612, L137
Rice W. K. M., Wood K., Armitage P. J., Whitney B. A., Bjorkman J. E., 2003, MNRAS, 342, 79
Rice W. K. M., Armitage P. J., Wood K., Lodato G., 2006, MNRAS, 373, 1619
Shakura N. I., Sunyaev R. A., 1973, A&A, 24, 337
Shu F. H., Shang H., Glassgold A. E., Lee T., 1997, Sci, 277, 1475
Varnière P., Blackman E. G., Frank A., Quillen A. C., 2006, ApJ, 640, 1110
Ward W. R., 1991, Lunar Planet. Sci. Conf., 22, 1463
Ward W. R., 1997, Icarus, 126, 261
Weidenschilling S. J., 1977, MNRAS, 180, 57

This paper has been typeset from a TEX/LATEX file prepared by the author.